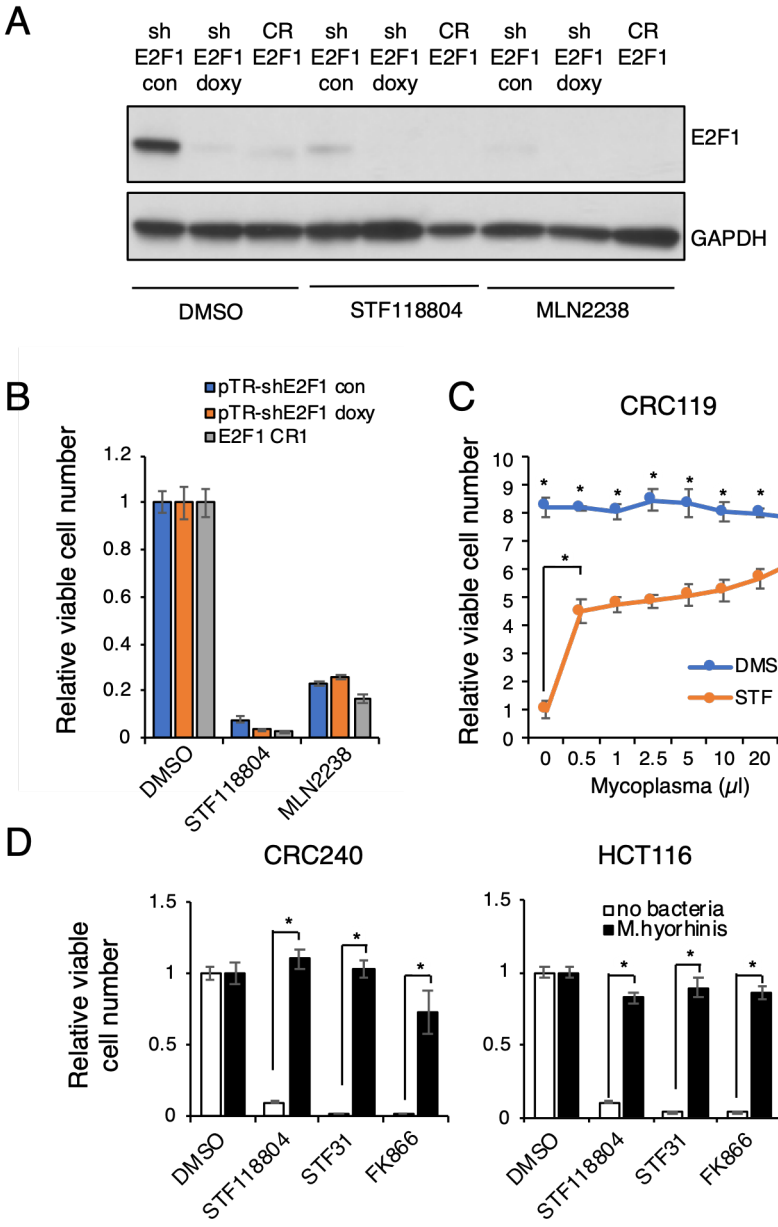

Figure S1. Mycoplasma infection rather than E2F1 knockdown protects mammalian host cells from toxicity induced by NAMPT inhibitors, Related to Figure 1.

(A-B) E2F1 knockdown does not affect sensitivity to STF118804, MLN2238. E2F1 was knocked down in CRC240 cells either using a doxycycline-inducible shRNA (doxy) or CRISPR/cas9 genome editing (CR). Cells were treated with 100 nM STF118804 or 100 nM MLN2238 for 41 hours. E2F1 protein levels were analyzed by Western blot (A) and cell viability was measured by CTG assay (B). (n=3, values are expressed as mean ±SD).

(C) Mycoplasma dose-dependently protect cells from STF-induced cell toxicity. Mycoplasma from 40 ml culture were spun down and resuspended in 1 ml PBS. Indicated volumes were added per well of 96 well plate with 100 ul containing 10,000 CRC119. Cells were then treated with DMSO control or 100 nM STF118804 for 48 hours. Cell viability was measured by CTG assay (n=3, values are expressed as mean ±SD, *p<0.05).

(D) Mycoplasma protect from toxicity induced by NAMPT inhibitors in additional cell lines. CRC240 and HCT116 colon cancer cell lines either without bacteria or chronically infected with *M. hyorhinis* were treated with three different NAMPT inhibitors (100 nM STF118804, 1 μM STF31 or 40 nM FK866) for 48 hours. Cell viability was measured by CTG assay (n=3, values are expressed as mean ±SD, *p<0.05).

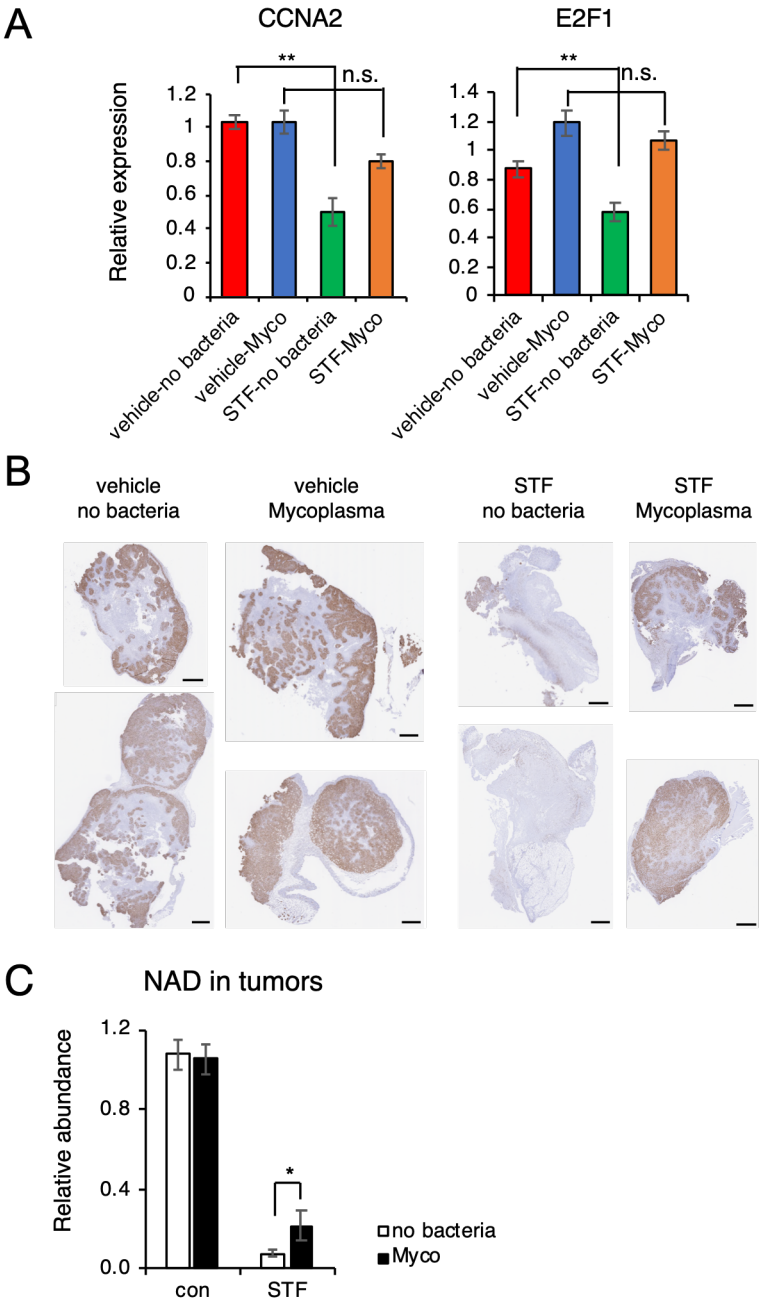

Figure S2. Mycoplasma attenuate STF118804-induced repression of proliferation markers in vivo, Related to Figures 1 and 2.

(A) Mycoplasma prevent repression of proliferation genes by STF118804. Clean (no bacteria) or M. hyorhinis-infected (Mycoplasma) HCT116 cells were xenografted into nude mice, then treated with 15 mg/Kg STF118804 or vehicle control as described in STAR Methods. The mRNA levels of Cyclin A2 (CCNA2) and E2F1 in xenograft tumors were quantified by qPCR (n=5-6, values are expressed as mean ±SEM, **p<0.01).

(B) Mycoplasma infected tumors are more resistant to STF118804-induced inhibition of cell proliferation than clean tumors. Xenograft tumors described in (A) were stained for a cell proliferation marker, Ki67. Bars, 1 mm.

(C) Mycoplasma infected tumors have an increased NAD content after STF118804 treatment compared to clean tumors. NAD content in xenograft tumors described in (A) was analyzed by LC-MS (n=6-7, values are expressed as mean ±SEM, *p<0.05).

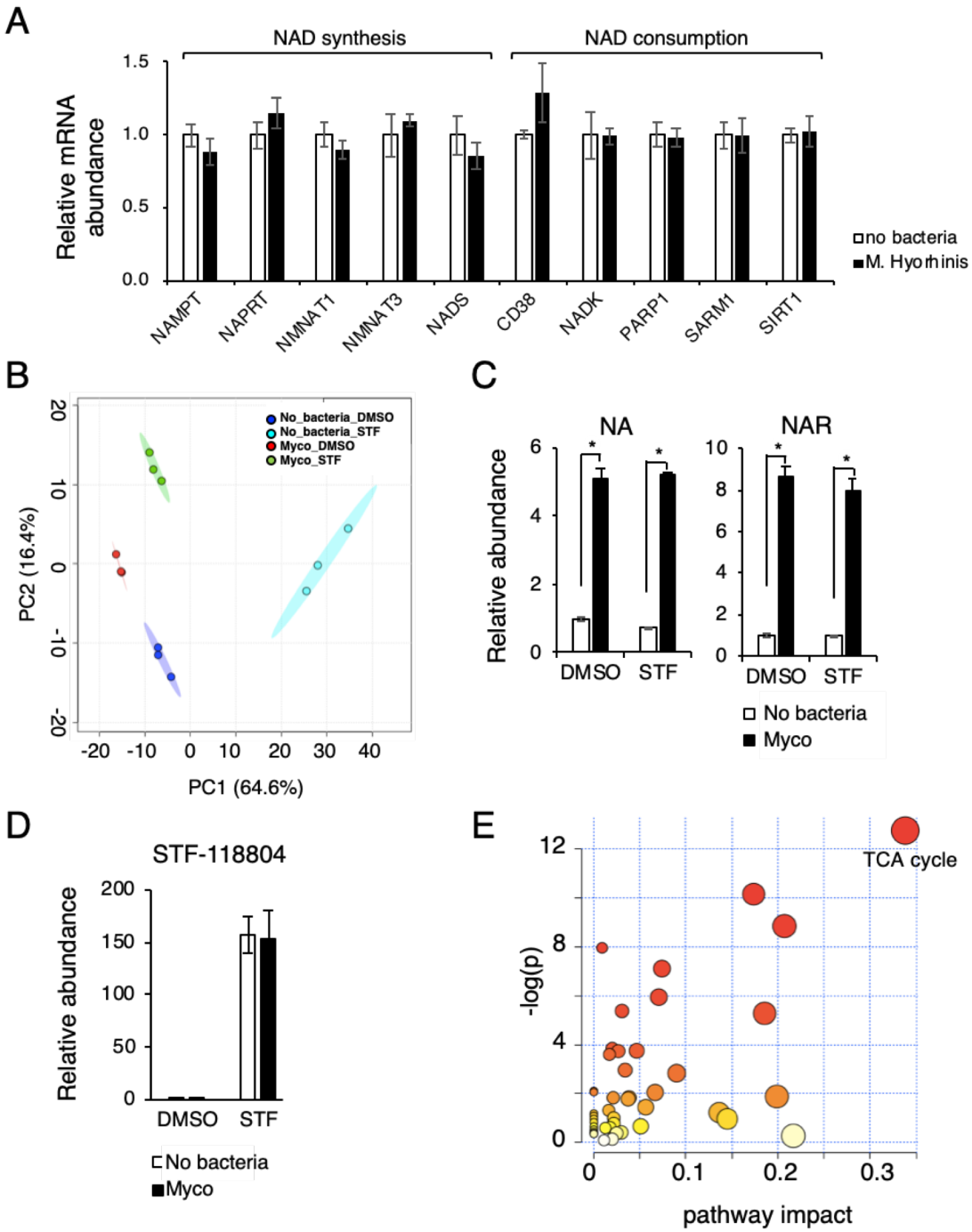

Figure S3. Metabolomics of CRC119 cells infected with M. hyorhinis, Related to Figure 3.

(A) Mycoplasma infection does not affect the expression of key NAD metabolic genes in human cells. Expression of the indicated NAD synthesis and consumption genes was analyzed in control and mycoplasma-infected cell by qPCR (n=3, values are expressed as mean ±SD).

(B) Principal component analysis of all significantly altered metabolites in clean and mycoplasma infected cells treated with or without STF118804.

(C) Mycoplasma elevate the concentration of Nicotinic acid (NA) and Nicotinic acid riboside (NAR) in the culture medium. Metabolites were analyzed by LC-MS (n=3, values are expressed as mean ±SD, *p<0.05).

(D) Mycoplasma do not affect the intracellular levels of STF118804. Relative abundance of intracellular STF-118804 was analyzed by LC-MS (n=3, values are expressed as mean ±SD).

(E) The TCA cycle is the most significantly altered metabolic pathway induced by mycoplasma in STF118804-treated cells (n=3). Metabolites that were significantly changed by mycoplasma infection in STF118804-treated cells were subjected to pathway analysis by MetaboAnalyst 3.0 (n=3, p<0.05).

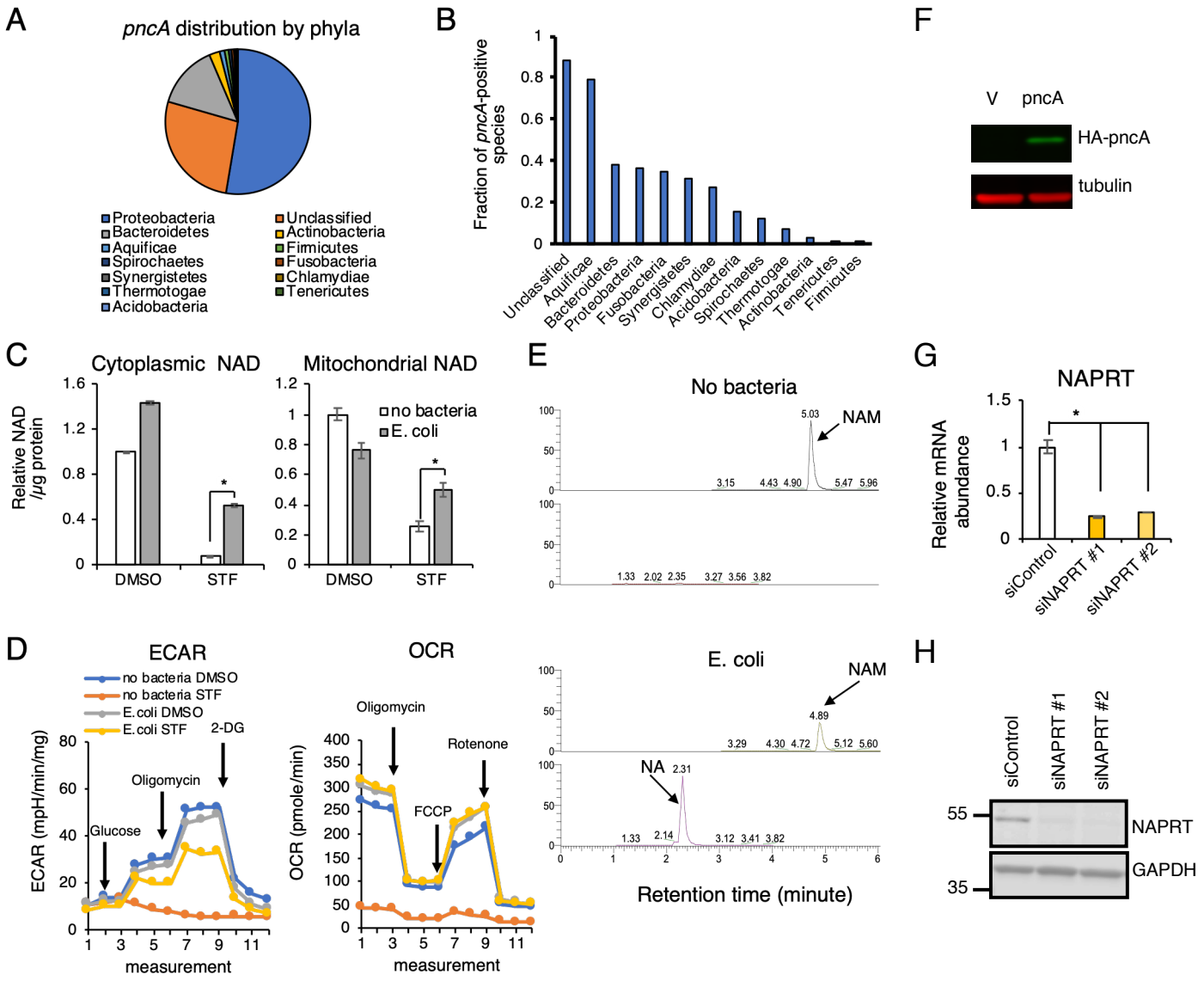

Figure S4. E. coli rescue NAMPTi-induced toxicity through pncA, Related to Figure 4.

(A) pncA is an ubiquitous enzyme encoded by diverse bacteria. 2088 bacterial proteins homologous to PncA were identified by domain search as described in STAR Methods. The full list of identified PncA homologs is available in Table S5. The pie chart represents the breakdown of absolute numbers of 2088 pncA-encoding bacterial species by phylum.

(B) Proportion of *pncA*-positive species varies widely across bacterial phyla. Absolute numbers of pncA homologs for each phylum were normalized to total number of analyzed sequenced species from that phylum.

(C) *E. coli* rescue STF118804-mediated depletion of cytoplasmic and mitochondrial NAD. CRC119 cells were treated with 100 nM STF18804 or DMSO control with or without 1:1000 dilution of overnight *E. coli* culture in the presence of 1 µg/ml gentamycin for 22 hours. Relative levels of total NAD (NADH + NAD+) were measured in isolated cytoplasmic and mitochondrial fractions by a colorimetric enzymatic assay and normalized to total protein (n=3, values are expressed as mean ±SD, *p<0.05).

(D) *E. coli* rescue STF118804-mediated shutdown of energy metabolism. CRC119 cells were infected with 1:1000 dilution of overnight *E. coli* culture (with 1 µg/ml gentamycin) or with control medium and cells were treated with 100 nM STF118804 or DMSO control. Seahorse analysis using Glycolysis Stress Test or Mito Stress Test was performed 40 hr later. Raw ECAR readings were normalized to total protein content (n=3, values are expressed as mean ±SD).

(E) *E. coli* induce the conversion of NAM to NA in culture medium. Representative chromatograms from the LC-MS analysis of NAM-containing RPMI medium after two hours of incubation at 37 degrees with or without *E. coli*. Bacteria were removed by centrifugation and filtering prior to the analysis.

(F) Overexpression of *E. coli* pncA in CRC119 cells. Western blot of HA-PncA and alpha tubulin loading control.

(G) Knockdown of NAPRT by siRNAs. CRC119 cells were transfected with a control siRNA or two independent siRNAs against NAPRT (siNAPRT #1 and siNAPRT #2). The relative abundance of NAPRT mRNA was analyzed by qPCR (n=3, values are expressed as mean ±SD, *p<0.05).

(H) The protein levels of NAPRT are reduced by siRNAs. CRC119 cells were treated as in (G) and NAPRT protein levels were analyzed by immunoblotting. GAPDH served as a loading control.

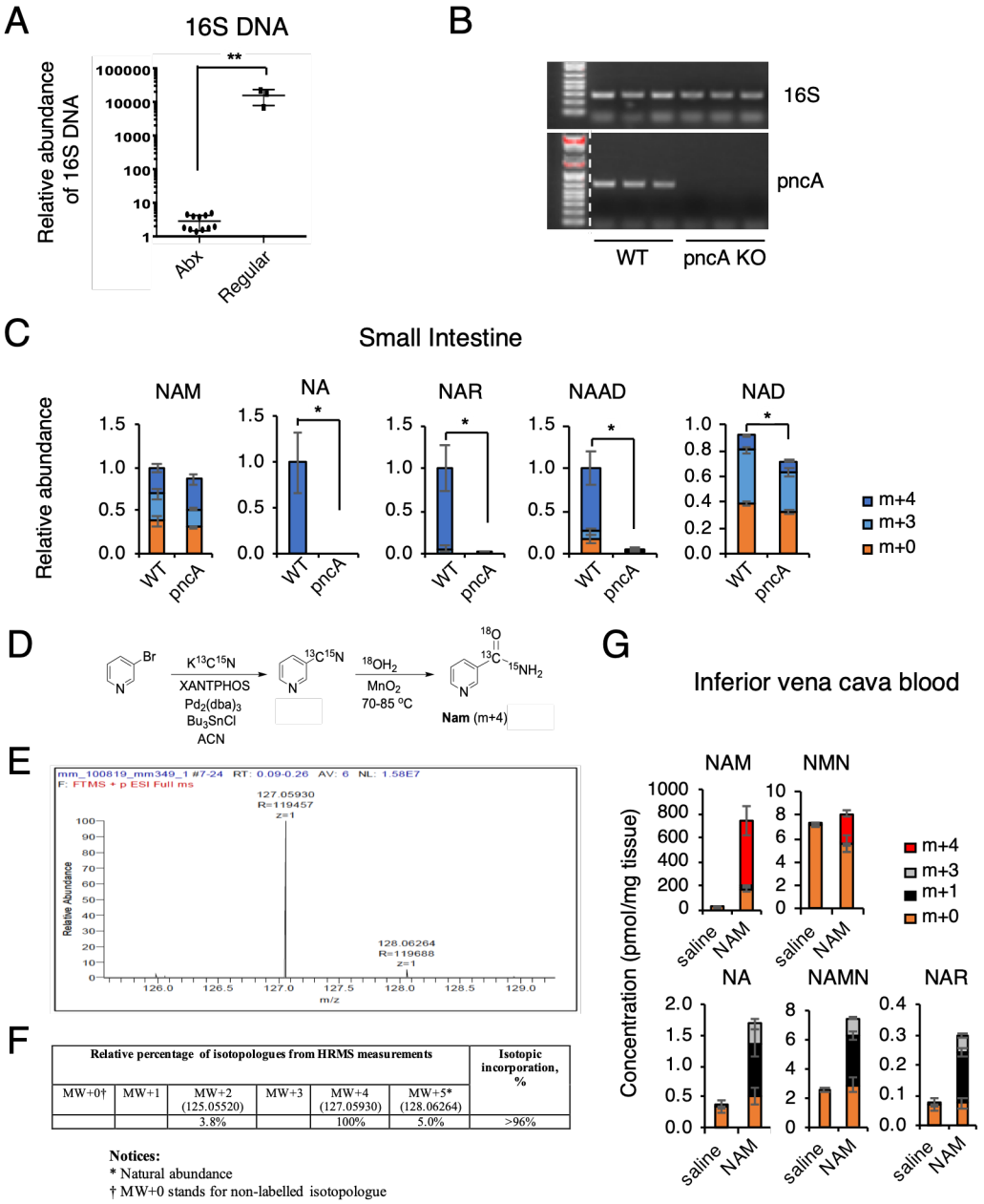

Figure S5. Oral NAM supplement is incorporated into NAD primarily through gut microbiota-enabled deamidated NAD biosynthesis pathway, Related to Figures 5 and 6.

(A) Depletion of gut microbiota in mice by antibiotic treatment. qPCR analysis of 16S rDNA in fecal DNA of mice used in the experiment described in Figure 5A-D. All microbiota-depleted mice and three representative conventional mice were analyzed (n=3-11 mice/group, values are expressed as mean ±SD, **p<0.01).

(B) Repopulation of germ free mice with WT or pncA KO *E. coli*. Germ-free mice were gavaged daily with $2x10^8$ cfu of WT or pncA KO *E. coli* for three days. Feces of gavaged mice were collected 4 days later and the levels of 16S rDNA and pncA genes in fecal DNA were analyzed by PCR (n=3 mice/group).

(C) *pncA* is required to incorporate oral NAM into metabolites in the deamidated NAD biosynthesis pathway in the small intestine. Germ-free mice repopulated with WT or pncA KO *E. coli* were orally gavaged with 80 mg/kg of D4-NAM and dissected three hours later. The relative abundance of unlabeled (m+0) and labeled (m+3 and m+4) NAD pathway metabolites in small intestine were measured by LC-MS (n=5-6 mice/group, values are expressed as mean ±SEM, *p<0.05).

(D) Synthesis of [^{18}O,^{15}N,^{13}C-*amide*]nicotinamide (^{18}O,^{15}N,^{13}C-NAM).

(E) HRMS data for ^{18}O,^{15}N,^{13}C-NAM (m+4).

(F) Isotopic incorporation for ^{18}O,^{15}N,^{13}C-NAM (NAM, MW+4) according to HRMS measurements.

(G) NAMN is the major deamidated NAM precursor in systemic blood. Regular mice were gavaged with 80 mg/kg of ^{18}O,^{15}N,^{13}C-NAM and the concentration of unlabeled (m+0) and labeled NAD pathway metabolites synthesized via the deamidated (m+3 and m+1) and amidated (m+4) pathways in blood collected from the inferior vena cava were measured by LC-MS 3 hours after gavage as described in Methods (n=3 mice/group, values are expressed as mean ±SEM).

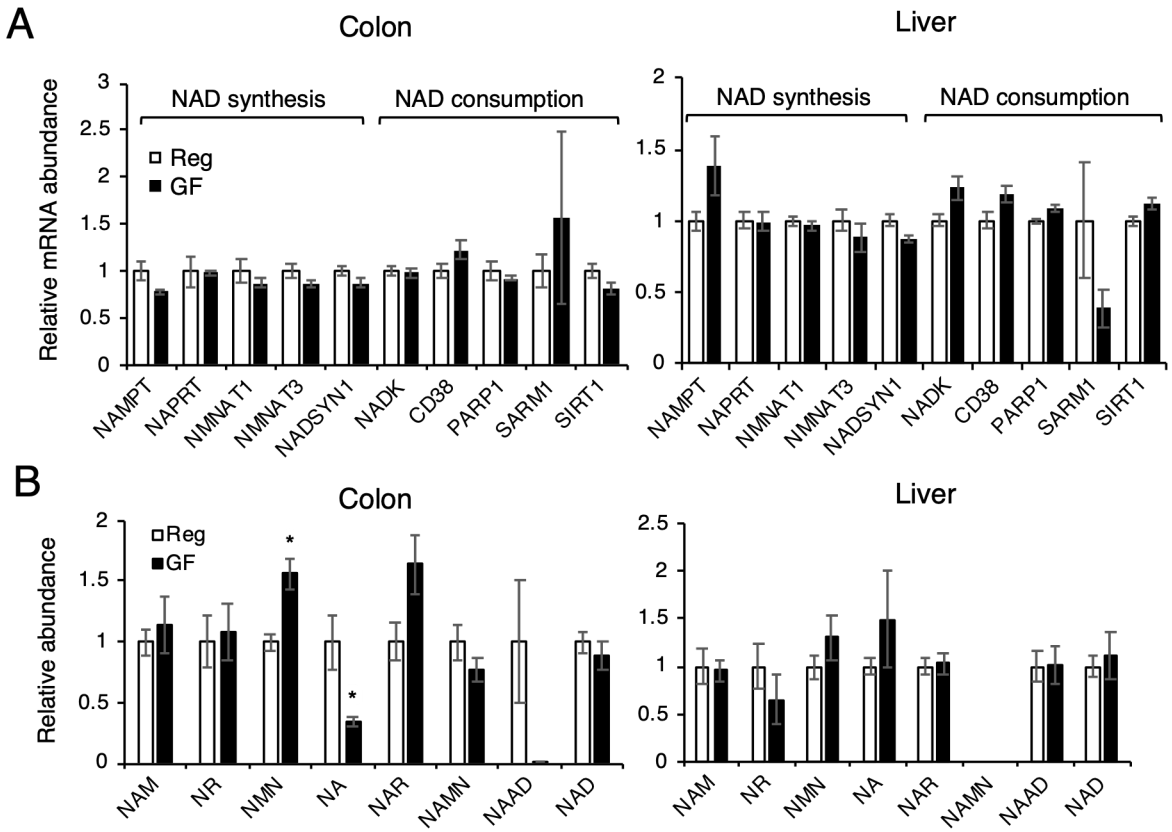

Figure S6. NAD metabolism in germ-free mice. Related to Figure 7.

(A) Germ-free mice have normal expression of key NAD metabolic genes in colon and liver. Expression of indicated NAD synthesis genes and NAD consumption genes were analyzed in colons and livers of control (Reg) and germ-free (GF) mice by qPCR (n=3-4 mice/group, values are expressed as mean ±SEM). There was no statistically significant differences in the expression of any of the genes between the two groups.

(B) Germ-free mice have reduced NA but increased NMN levels in colon. The relative abundance of indicated NAD metabolites in colon and liver of saline-gavaged control (Reg) and germ-free (GF) mice were analyzed by LC-MS (n=3-4 mice/group, values are expressed as mean ±SEM, *p<0.05).

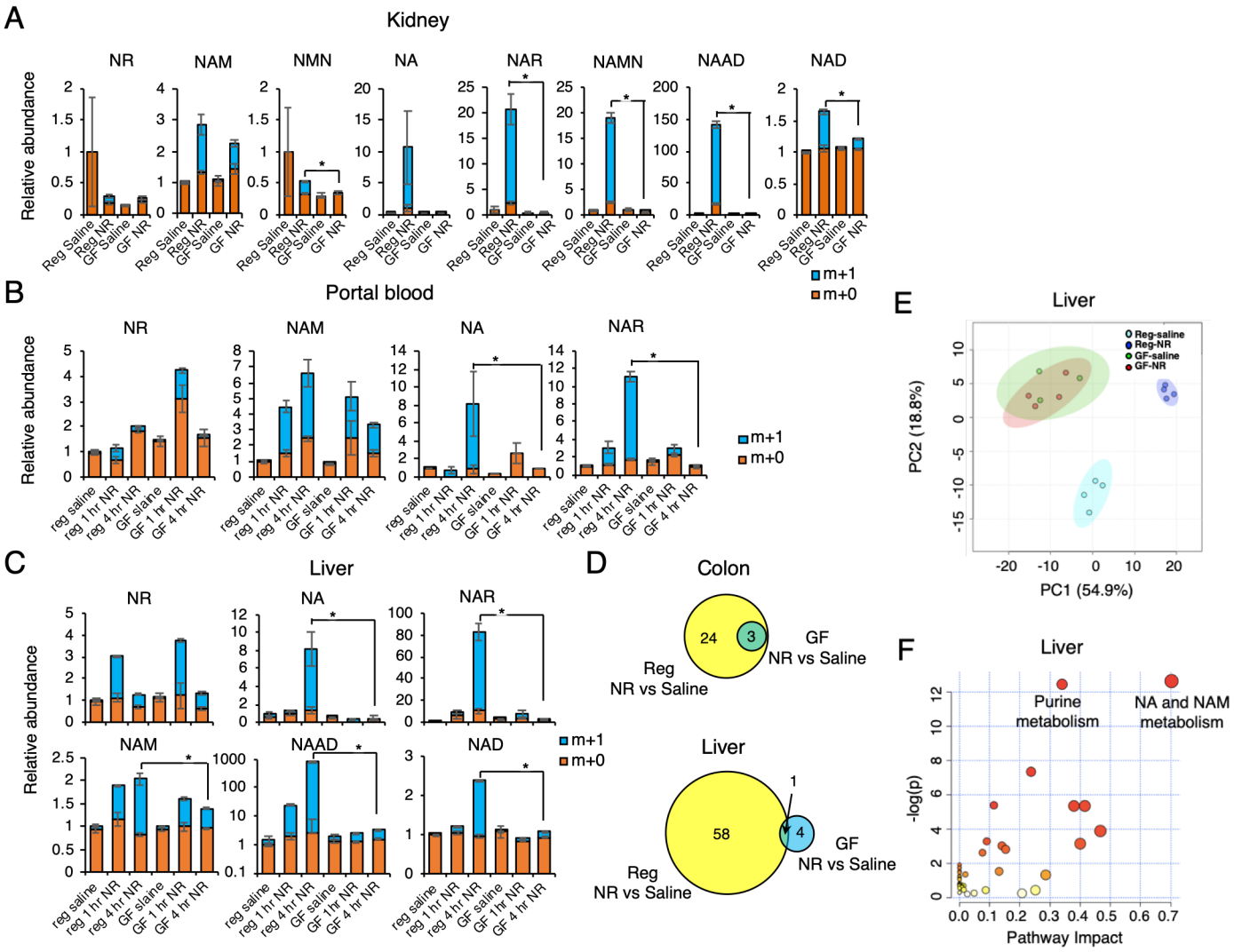

Figure S7. Gut microbiota plays an important role in incorporation of dietary NR into deamidated precursors and NAD *in vivo*, Related to Figure 7.

Regular (Reg) and germ-free (GF) C57BL/6NTac mice were gavaged with 185 mg/kg of *pyridyl*-^{15}N-labeled NR chloride or with saline control, and dissected one or four hours later. The relative abundance of small molecular metabolites in portal blood, colon and liver were analyzed by LC-MS.

(A) Gut microbiota plays an important role in incorporation of dietary NR into NAD through both amidated and deamidated pathways in kidney. Relative abundance of unlabeled (m+0) and labeled (m+1) metabolites in NAD metabolic pathways were measured by LC-MS 4 hours after NR gavage in kidney (n=3-4 mice/group, values are expressed as mean ±SEM, *p<0.05). The LC-MS analysis was done as described in Methods under NIEHS LC-MS.

(B) Gut microbiota-produced amidated and deamidated NAD precursors from dietary NR are detectable in the portal blood. Relative abundance of unlabeled (m+0) and labeled (m+1) NAD pathway metabolites in the portal blood were measured at 1 or 4 hours after NR gavage (n=3-4 mice/group, values are expressed as mean ±SEM, *p<0.05). The LC-MS analysis was done as described in Methods under NIEHS LC-MS.

(C) Gut microbiota plays an important role in incorporation of dietary NR into hepatic NAD through deamidated pathway. Relative abundance of unlabeled (m+0) and labeled (m+1) hepatic metabolites in the NAD biosynthesis pathways were measured by LC-MS at 1 or 4 hours after NR gavage (n=3-4 mice/group, values are expressed as mean ±SEM, *p<0.05). The LC-MS analysis was done as described in Methods under NIEHS LC-MS. These results confirm those presented in Figure 6E, which were collected in an independent lab using Duke LC-MS method.

(D) Germ-free mice do not display NR-induced metabolic alterations in the colon and the liver. Venn diagrams represent numbers of significantly changed metabolites (p<0.05) in colons and livers of NR-gavaged mice compared with saline-treated controls (4 hours after the treatment).

(E) Germ-free mice are non-responsive to NR-induced metabolic alterations in the liver. The total detectable metabolites in livers at four hours after gavage with NR or saline were analyzed by principal component analysis.

(F) Metabolic changes in the livers of regular mice after NR gavage. Liver metabolites that were significantly changed after four hours of NR gavage in regular mice were subjected to pathway analysis by MetaboAnalyst 3.0 (n=3-4 mice/group, p<0.05). As expected, NA and NAM metabolism is the most significantly affected pathway followed by purine metabolism.